Article
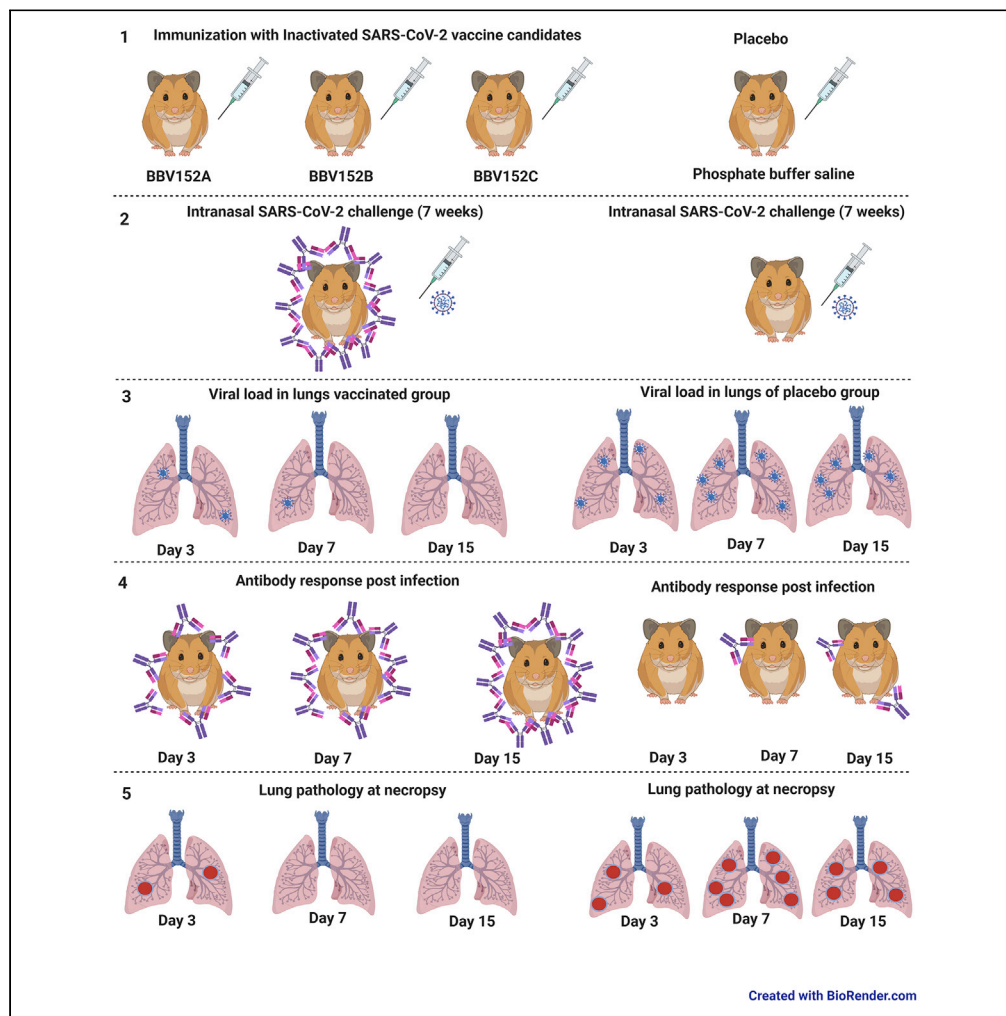
Immunogenicity and protective efficacy of BBV152, whole virion inactivated SARS- CoV-2 vaccine candidates in the Syrian hamster model

Created with BioRender.com

Sreelekshmy
Mohandas, Pragya
D. Yadav, Anita
Shete-Aich, ...,
Krishna M. Ella,
Samiran Panda,
Balram Bhargava

hellopragya22@gmail.com

HIGHLIGHTS

Vaccine candidates,
BBV152 induced potent
humoral immune
response in Syrian
hamsters

Early viral clearance from
lower respiratory tract in
vaccinated hamsters

BBV152 vaccine
candidates protected
Syrian hamsters from
pneumonia

iScience

Article

Immunogenicity and protective efficacy of BBV152, whole virion inactivated SARS- CoV-2 vaccine candidates in the Syrian hamster model

Sreelekshmy Mohandas,[1] Pragya D. Yadav,[1,5,*] Anita Shete-Aich,[1] Priya Abraham,[1] Krishna Mohan Vadrevu,[2] Gajanan Sapkal,[1] Chandrashekhar Mote,[3] Dimpal Nyayanit,[1] Nivedita Gupta,[4] Vellimedu Kannappa Srinivas,[2] Manoj Kadam,[1] Abhimanyu Kumar,[1] Triparna Majumdar,[1] Rajlaxmi Jain,[1] Gururaj Deshpande,[1] Savita Patil,[1] Prasad Sarkale,[1] Deepak Patil,[1] Raches Ella,[2] Sai D. Prasad,[2] Sharda Sharma,[1] Krishna M. Ella,[2] Samiran Panda,[4] and Balram Bhargava[4]

SUMMARY

The availability of a safe and effective vaccine would be the eventual measure to deal with severe acute respiratory syndrome coronavirus-2 (SARS-CoV-2) threat. Here, we have assessed the immunogenicity and protective efficacy of inactivated SARS-CoV-2 vaccine candidates BBV152A, BBV152B, and BBV152C in Syrian hamsters. Three dose vaccination regimes with vaccine candidates induced significant titers of SARS-CoV-2-specific IgG and neutralizing antibodies. BBV152A and BBV152B vaccine candidates remarkably generated a quick and robust immune response. Post-SARS-CoV-2 infection, vaccinated hamsters did not show any histopathological changes in the lungs. The protection of the hamster was evident by the rapid clearance of the virus from lower respiratory tract, reduced virus load in upper respiratory tract, absence of lung pathology, and robust humoral immune response. These findings confirm the immunogenic potential of the vaccine candidates and further protection of hamsters challenged with SARS-CoV-2. Of the three candidates, BBV152A showed the better response.

INTRODUCTION

Since the first report in December 2019, severe acute respiratory syndrome coronavirus-2 (SARS-CoV-2) has spread at an alarming rate. It has infected more than 55.3 million people with about 1.3 million cases succumbed to the disease across 220 countries and territories around the world until 18 November 2020 (World Health Organization, 2020a). Globally, scientific communities are actively engaged and trying to develop suitable vaccine candidates and specific antiviral therapies against this virus. Vaccination is the most significant pharmaceutical intervention for the prevention of any infectious disease impacting the health of communities worldwide. Accelerated efforts are being taken for the development of a safe and effective vaccine worldwide which is evident by the number of vaccine candidates under preclinical and clinical evaluation. According to the World Health Organization draft landscape document on COVID-19 candidate vaccines published on 3rd November 2020, 47 vaccine candidates are under clinical and 155 under preclinical studies (World Health Organization, 2020b).

SARS-CoV-2 is an enveloped, single-stranded, positive-sense RNA virus that belongs to the genus *Betacoronavirus* of the family *Coronaviridae*. There are other coronaviruses known to infect humans like human coronavirus (HCoV) 229E and NL63 (Alphacoronavirus), HCoV-OC43, HKU1, SARS-CoV, and Middle East respiratory syndrome coronavirus (MERS-CoV) (*Betacoronavirus*). Although the reported mortality of COVID-19 is less compared to the SARS and MERS, the rate of transmission is much higher than these viruses (Wilder-Smith, et al., 2020). The disease has an overall case fatality rate of 0.5%–2.8% with higher rates i.e. 3.7–14.8% in elderly patients (The Center for Evidence-Based Medicine, 2020).

The origin of SARS-CoV-2 seems to be from bat, while the role of intermediate host is still debatable (Docea, et al., 2020). SARS-CoV-2 is usually transmitted through droplets and contact with contaminated

[1]Indian Council of Medical Research-National Institute of Virology, Sus Road, Pashan, Pune, Maharashtra 411021, India

[2]Bharat Biotech International Limited, Genome Valley, Hyderabad, Telangana 500 078, India

[3]Department of Veterinary Pathology, Krantisinh Nana Patil College of Veterinary Science, Shirwal, Maharashtra 412801, India

[4]Indian Council of Medical Research,V. Ramalingaswami Bhawan, P.O. Box No. 4911, Ansari Nagar, New Delhi 110029, India

[5]Lead Contact

*Correspondence: hellopragya22@gmail.com

https://doi.org/10.1016/j.isci.2021.102054

surfaces (Phan et al., 2020). Adults and elderly individuals with history of respiratory diseases, metabolic diseases and weaker immune system are more prone to the disease (Tsatsakis, et al., 2020). Additionally, there are many factors like environmental factors, societal customs, and personal hygiene which can aid in the spread of SARS-CoV-2 (Goumenou, et al., 2020). On an average, symptomatic cases can transmit the infection to three people. However, the virus can be also be transmitted during the early phase of illness when the patients are asymptomatic (Li, et al., 2020).

The incubation period of COVID-19 ranges from 2 to 14 days with a median period of 5 days. It is characterized by mild to severe illness with signs and symptoms such as fever, dry cough, vomiting, diarrhea, myalgia, dyspnea, and pulmonary infiltrates (Tsatsakis, et al., 2020). There are no approved antiviral drugs available for the treatment of COVID-19. The mild cases are treated symptomatically, and severe cases are managed with intensive care interventions. Recently, the use of remdesivir for the treatment of COVID-19 cases has been authorized by the US Food and drug organization under Emergency Use Authorization. However, it is yet to be given not complete approval (Islam, et al., 2020). Considering the pandemic's nature and dreadful scenario of COVID-19, vaccines will be the most appropriate and effective intervention for controlling the rapid spread of this disease.

Currently along with the conventional vaccine development platforms, advanced technologies are being used for the development of vaccines against SARS-CoV-2 like messenger RNA, DNA, viral vectors, recombinant sub-unit proteins, virus-like particles, etc (Pandey et al., 2020). Despite the advances in vaccine design technologies, the development of an inactivated vaccine remains the most simple and relatively less expensive approach to produce a safe and effective vaccine. Inactivated vaccines have been used effectively to curb many infectious diseases in the past (Sanders et al., 2015). Recently, two inactivated SARS-CoV-2 vaccine candidates have shown promising results in preclinical trials (Gao et al., 2020; Wang et al., 2020).

Multiple animal models have been used to evaluate the efficacy of SARS-CoV-2 vaccine candidates. Syrian hamster (*Mesocricetus auratus*) is one such model which has been used in diverse research studies on SARS-CoV-2 and seems to be the appropriate model as it mimics the human disease in comparison to other animals (Mohandas et al., 2020; Luan et al., 2020; Chan et al., 2020; Imai et al., 2020; Wang et al., 2019; Sia et al., 2020). Moreover, high binding affinity of SARS-CoV-2 spike glycoprotein receptor-binding domain to hamster ACE2 has been predicted with in silico structural analysis (Chan et al., 2020). The study on the SARS-CoV-2 pathogenesis in hamsters demonstrated the pulmonary pathology and high lung viral load during the first week of infection (Chan et al., 2020). Similarly, our study among various small laboratory animal models demonstrated effective SARS-CoV-2 replication in the upper and lower respiratory tract of hamsters compared to mice (Mohandas et al., 2020). Besides this, Syrian hamsters have been successfully used to evaluate medical countermeasures for SARS-CoV-2 by multiple research groups (Luan et al., 2020; Chan et al., 2020; Imai et al., 2020; Rogers et al., 2020; Tostanoski et al., 2020).

We have developed three whole virion inactivated vaccine candidates BBV152A [3μg + Aluminum hydroxide (Algel)-Imidazoquinoline (IMDG)], BBV152B (6μg + Algel-IMDG) and BBV152C (6μg + Algel) using β-propiolactone inactivation method. The vaccine candidates along with Algel adjuvant alone or with Algel chemisorbed with IMDG was found to be immunogenic and safe in the preclinical studies on laboratory mice, rats, and rabbits (Ganneru et al., 2020). Here, we report the immunization of Syrian hamsters with these vaccine candidates and evaluation of protective efficacy against SARS-CoV-2 by carrying out virus challenge experiment in immunized hamsters.

RESULTS

Optimization of SARS-CoV-2 challenge dose in Syrian hamsters

For assessment of the SARS-CoV-2 challenge dose after immunization, a 10-fold serial dilutions of $10^{5.5}$ median tissue culture infectious dose ($TCID_{50}$) were used. One hundred microliter (μL) from each of the 5 dilutions ($10^{5.5}$, $10^{4.5}$, $10^{3.5}$, $10^{2.5}$, and $10^{1.5}$) was inoculated intranasally in 5 groups of 6 hamsters each. On 3 day post-infection (DPI), 3 hamsters each from all the 5 groups were sacrificed and the lung viral titers were measured. Virus load was found to be similar in all the hamsters by real-time Reverse transcription-Polymerase Chain Reaction (RT-PCR) irrespective of the virus dilutions inoculated. Further to confirm this finding, virus titration was performed on the same lung samples and $TCID_{50}$ titer ranging between $10^{5.48}$ and $10^{5.58}$ was observed in all samples on 3 DPI (Figure S1). Similarly on day 14, the remaining hamsters were sacrificed and lung samples were found to show a titer of $10^{2.5}$ $TCID_{50}$/ml in all the animals, indicating
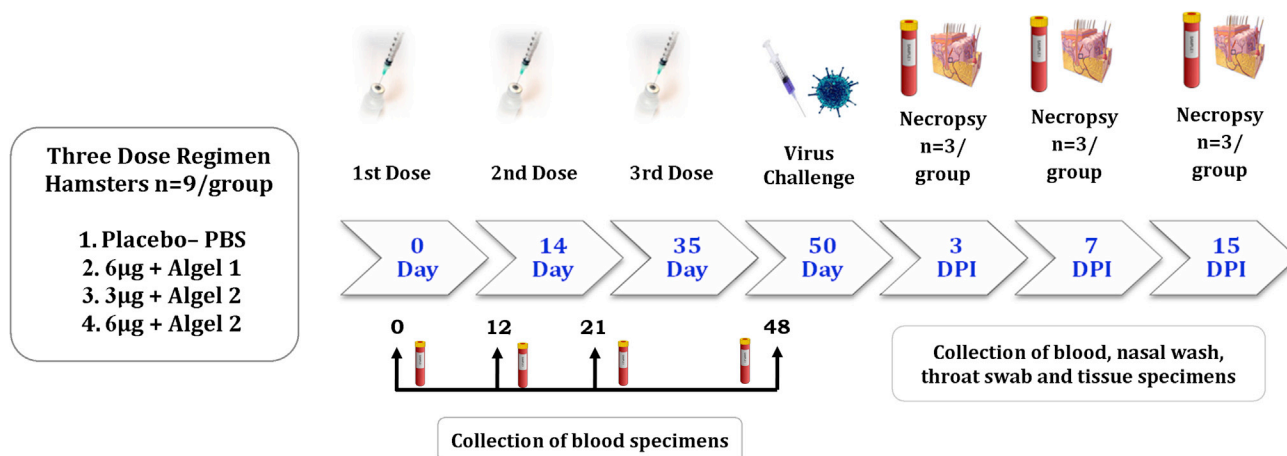
Figure 1. Schematic presentation of experiments in hamsters

Three doses of placebo were administered to the first group of the animals which were controls in the study. Three different inactivated SARS-CoV-2 vaccine formulations (2 doses + boost) were administered to the three groups of animals. All the animals were challenged at 15 days after the third dose. Samples were collected at different time points of immunization period and post-infection as indicated in the figure. Necropsy was performed for three hamsters from each group at 3, 7, and 15 DPI.

that viral inoculums could induce disease in all hamsters (Figure S1). On histopathological analysis, lungs samples of the hamsters inoculated with the $10^{5.5}$ $TCID_{50}$ and $10^{4.5}$ $TCID_{50}$ dilutions collected on 3DPI showed mild inflammatory changes indicating beginning of pneumonia, whereas other groups showed minimal or no changes. On 14 DPI, the lung pathological changes were found minimal in all groups indicating recovery from infection. Even though the lung viral titers in all groups were similar irrespective of the dose of virus inoculums, the lung pathological changes indicated the rapid induction of pneumonic changes in $10^{5.5}$ and $10^{4.5}$ dilutions. Hence, a virus dilution dose of $10^{5.5}$ TCID50 was used for virus challenge.

Clinical observations during BBV152A, BBV152B, and BBV152C immunization period and after SARS-CoV-2 challenge

We immunized four groups of 6–8-week-old Syrian hamsters (9 hamsters in each group), with phosphate buffered saline (group I), BBV152C (group II), BBV152A (group III), and BBV152B (group IV) (Figure 1) with two doses on day 0 and 14. All the hamsters received one more booster dose on day 35. Rectal temperature remained within the normal range, and no clinical signs were observed in all the groups throughout the immunization period. The body weight increased until 7 weeks post-immunization (Figure 2A) but following SARS-CoV-2 infection on day 50, a decrease in body weight was observed in all the groups (Figure 2B). However, the percentage decrease in vaccinated groups were lesser compared to the group I. The decrease in body weight of group III hamsters was less as compared to other groups (Figure 2B).

Inactivated whole virion vaccine candidates BBV152A, BBV152B, and BBV152C induced specific IgG/neutralizing antibody

Anti-SARS-CoV-2 IgG antibody response was detected by third week in 8 of 9 hamsters of group IV with an average optical density (OD) of 0.62, 8 of 9 hamsters in group III with an average OD of 0.42 and in 2 of 9 hamsters (average OD = 0.285) of group II. On day 48, IgG antibody response was found to be increasing in the vaccinated groups with an average OD of 1.32 in group IV (9 of 9 hamsters), 1.2 in group III (9 of 9 hamsters) and 0.55 in group II (9 of 9 hamsters) (Figures 3A and 3C). All the animals in group I remained negative for IgG antibody during immunization period, whereas after virus challenge, 2 of 3 hamsters showed IgG positivity by 7 DPI and 3 of 3 by 14 DPI (average OD = 0.29) in the group I (Figure 3B). In the vaccinated groups, an increasing trend with an average OD of 0.84, 0.97, and 0.91 was observed on days 3, 7, and 15 DPI, respectively (Figure 3D). No significant difference was observed in the IgG antibody response post-infection in group III and IV.

IgG antibody response in vaccinated hamsters was further characterized to determine the IgG subclass profiles. On sub-typing, IgG2 was detected in all the IgG antibody positive samples, whereas it was
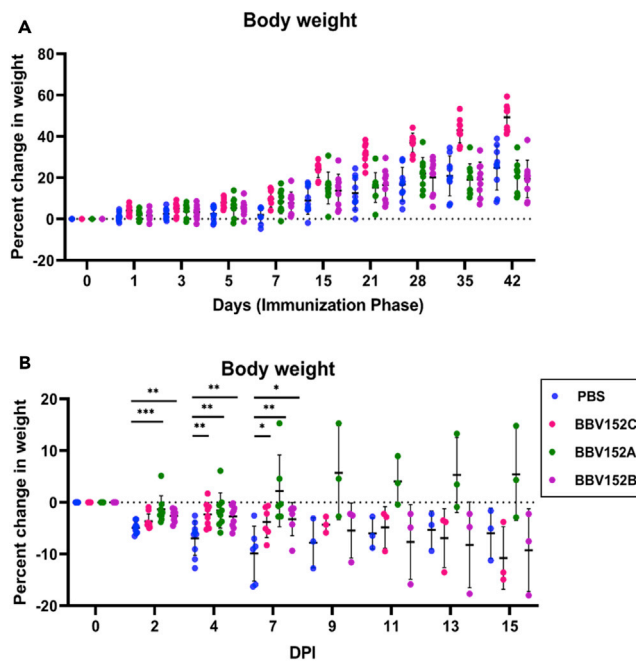
Figure 2. Percent body weight gain/loss in hamsters

(A) Percentage of body weight gain in hamsters during the immunization period.

(B) Percent difference in body weight in hamsters after SARS-CoV-2 challenge. Mean along with standard deviation (SD) is depicted in the scatterplot. The statistical significance was assessed using the Kruskal-Wallis test followed by the two-tailed Mann-Whitney test between the two groups; p values less than 0.05 were considered to be statistically significant.

negative for IgG1 during immunization and post-infection phase (Figure 3E). All three formulations of vaccine candidates significantly induced IgG2 with an increasing trend post-infection.

Neutralizing antibody (NAb) started appearing in the immunized groups at third week of immunization and increased till seventh week with highest titer (mean = 28,810) in group III (Figure 3F). After virus infection, the highest titer of NAb (mean = 85,623) was seen in group III animals on 15 DPI. Group I did not show NAb response during immunization phase and after virus infection till 15 DPI (Figure 3G).

Detection of SARS-CoV-2 genomic RNA (gRNA) in swabs/ organ samples after virus challenge in immunized animals

SARS-CoV-2 viral genomic RNA (gRNA) copy number in throat swabs (TSs) of group I were significantly higher than other groups on 3, 5, and 7 DPI (Figure 4A). The viral gRNA in group I persisted till 10 DPI, whereas it was cleared in all the vaccinated groups by 7 DPI. Higher copy numbers of viral gRNA were detected in the nasal washings of group I in comparison to immunized animals (Figure 4B).

Lungs (Figure 5A), nasal turbinates (Figure 5B), and trachea (Figure 5C) of group I showed higher viral gRNA copy number compared to immunized groups on 3 and 7 DPI. Trachea was cleared of viral gRNA by 7 DPI in all the vaccinated groups. Complete gRNA clearance was observed from lungs of group III and IV on 7 DPI and from group II by 15 DPI. Nasal turbinates viral gRNA persisted in all the groups till 15 DPI but with lower copy numbers in vaccinated groups compared to group I. No viral subgenomic (sg) RNA was detected in TS, nasal wash, nasal turbinate or trachea of animals of vaccinated groups. However viral sgRNA was detected in lungs (3/3), trachea (1/3), and nasal turbinate (1/3) in group I animals on 3 DPI. The spleen, kidney, and small intestine of hamsters of group I showed viral gRNA positivity on 3 DPI as well (Figure 5D).

Virus titration

Lungs and nasal turbinate samples of group I showed an average titer of 10^6 and $10^{5.5}$ TCID$_{50}$/ml, respectively, on 3 DPI. In the vaccinated groups III and IV, nasal turbinates showed an average titer of 10^5 and 10^4 TCID$_{50}$/ml on 3DPI, whereas the lungs titer was found considerably less ($10^{2.5}$TCID$_{50}$/ml) compared to
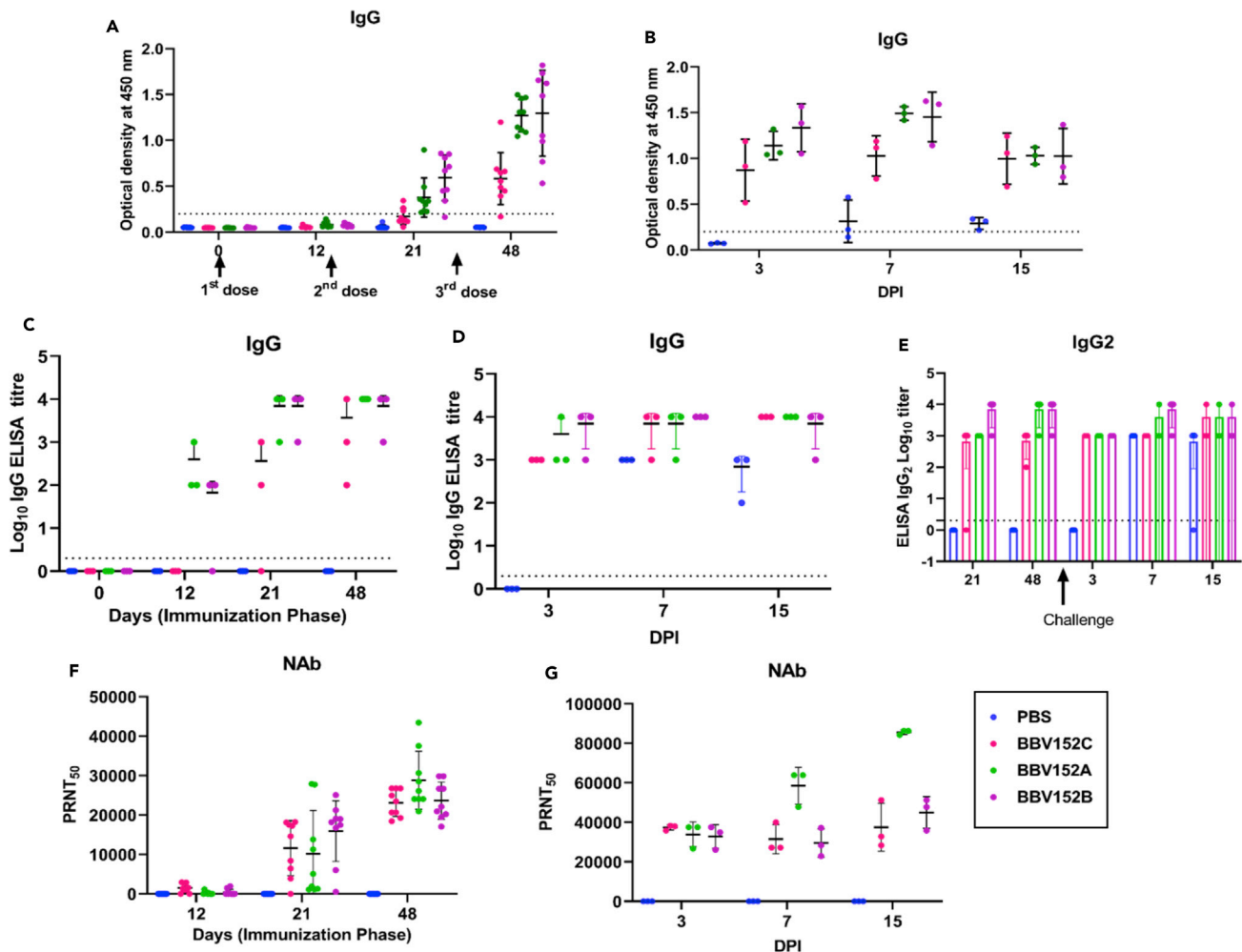
Figure 3. Humoral response in vaccinated animals

(A) IgG antibody response for all groups of animals observed on 12, 21, and 48 days.

(B) IgG antibody response at post-infection (3, 7, and 15 DPI) for all groups of animals.

(C) Comparison of IgG antibody titers between groups on 12, 21, and 48 days.

(D) Comparison of IgG antibody titers between groups after virus challenge at 3, 7, and 15 DPI.

(E). Comparison of IgG2 antibody titers between groups during immunization period at 21 and 48 days and post virus challenge at 3,7, and 15 DPI.

(F and G) (F). Comparison of NAb titers response during a three-dose vaccine regime for all groups of animals observed on 12, 21, and 48 days (G). Comparison of NAb titers response in SARS-CoV-2 infected animals on 3, 7, and 15 DPI. Mean along with standard deviation (SD) is depicted in the scatterplot. The statistical significance was assessed using the Kruskal-Wallis test followed by the two-tailed Mann-Whitney test between the two groups; p values less than 0.05 were considered to be statistically significant. The dotted lines indicate the limit of detection of the assay.

group I. In contrast, group II did not show live virus titer in any of the specimens on 3, 7, and 15 DPI. The samples of group II animals (n = 3) on 3 and 7 DPI were repeated for virus titration and also attempt was made for virus isolation, but in second passage in Vero CCL81 cells, the viral RNA presence was found negligible in samples showing that virus was not replicating in these samples. On 7 DPI, only nasal turbinates of group I showed virus titer, whereas vaccinated groups were negative. This correlates with the decreasing trend of gRNA and sgRNA in immunized groups after 3 DPI.

Pathological and immuno-histochemical findings in lungs after virus challenge

The lungs of the vaccinated groups appeared normal on 3, 7, and 15 DPI (Figures 6B, 6C, and 6D) grossly, whereas on 7 DPI, the lungs of group I showed diffuse areas of consolidation and congestion (Figure 6A). On histopathological examination, lung sections from group I animals showed congestion, haemorrhages, exudations in the alveoli, mononuclear cell infiltration in the alveolar interstitium, and pneumocyte
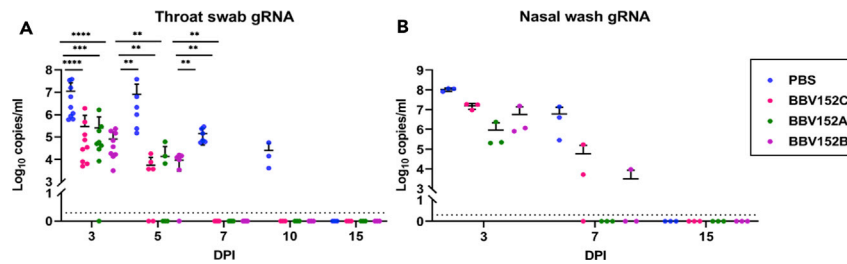
Figure 4. Log$_{10}$ plot for the genomic viral RNA detection in throat swab and nasal wash after virus challenge
Genomic viral RNA load in (A) Throat Swab collected at 3, 5, 7, 10, and 15 DPI for the all groups (B) Nasal wash genomic viral RNA at 3, 7, and 15 DPI for the all groups. Mean along with standard deviation (SD) is depicted in the scatterplot. The statistical significance was assessed using the Kruskal-Wallis test followed by the two-tailed Mann-Whitney test between the two groups; p values less than 0.05 were considered to be statistically significant. The dotted lines indicate the limit of detection of the assay.

hyperplasia on 3 and 7 DPI (Figures 6E and 6F). Occasionally, loss of bronchiolar epithelium was also observed. By 15 DPI, fibro-elastic proliferation with collagen deposition at alveolar epithelial lining were observed in the lungs of group I (Figure 6G). Vaccinated group animals did not show any histopathological evidence of pneumonia except few congestive foci on 3 DPI (Figures 6H, 6I, 6J, and S2). The viral antigen could be detected in alveolar type-II pneumocytes and macrophages on 3, 7, and 15 DPI in the lungs of group I animals (Figures 7A, 7B, and 7C), whereas only focal positivity was detected in the vaccinated groups on 3 DPI. On 7 and 15 DPI, viral antigen was not detected in the lung sections of vaccinated hamsters from all the groups on immunohistochemistry (Figures 7D, 7E, 7F, and S3).

Cytokine profile after virus challenge

After challenge with the virus, vaccinated groups did not show any significant elevation of cytokines i.e TNF-α, IL-4, IL-10, IL-6, IFN-γ, and IL-12, whereas in control group increased level of IL-12 was detected on 3 DPI which further reduced on 7 and 15 DPI (Figure S4).

DISCUSSION

Preclinical research in animal models is an important step in evaluating the immunogenicity and protective efficacy of vaccine candidates. Syrian hamster (*Mesocricetus auratus*) has been used in diverse research studies on SARS-CoV-2 and seems to be the appropriate model as it mimics the clinical signs, antibody response, viral kinetics, and histopathological changes of human disease (Chan et al., 2020; Luan et al., 2020; Mohandas et al., 2020; Imai et al., 2020; Wang et al., 2019). We performed a preliminary dose optimization study in Syrian hamsters for the experiment and observed that the viral RNA load in the lungs samples of infected hamsters did not show any difference with dose administered. Similar findings were reported with experimental inoculation of 10^3 or 10^5 TCID$_{50}$ of SARS-CoV and $10^{5.6}$ PFU or 10^3 PFU SARS CoV-2 in Syrian hamsters (Roberts et al., 2005; Imai et al., 2020) indicating the capability of virus to replicate to high titers in pulmonary tract, even at lower doses. We observed replication even at still lower doses of $10^{1.5}$ and $10^{2.5}$ TCID$_{50}$ than earlier reported studies.

The safety and immunogenicity profile of the vaccine candidates BBV152A, BBV152B, and BBV152C has been established in mice, rat, and rabbit models (Ganneru et al., 2020). Here, we report the immunogenicity and protective efficacy of these inactivated SARS-CoV-2 vaccine candidates in the hamster model. NAb are considered as a correlate of protection in SARS-CoV-2 infection in humans (Addetia et al., 2020). SARS-CoV-2 vaccination experiments in hamster and rhesus macaque models also indicated the same (Tostanoski et al., 2020; Yu et al., 2020). BBV152 induced SARS-CoV-2-specific IgG or NAbs in hamsters from third week post-immunization similar to the response observed in mice, rats, rabbits, and rhesus macaques (Ganneru et al., 2020; Yadav et al., 2020). In other SARS-CoV-2 inactivated vaccine candidates like PiCoVacc and BBIBP-CorV, studied in non-human primate model, the NAb were observed from first and second week, respectively, with a period of detection till 5 weeks (Gao et al., 2020; Wang et al., 2020). In the BBV152A, BBV152B, and BBV152C vaccinated groups, NAbs showed an increasing trend till 7 weeks and also after SARS-CoV-2 challenge (15 DPI). Although there was no statistically significant difference, group III showed the highest NAb titer after challenge i.e, a 2–3-fold rise compared to pre-challenge. Dose sparing effect of the antigen was evident in the NAb response after challenge by Algel + IMDG group
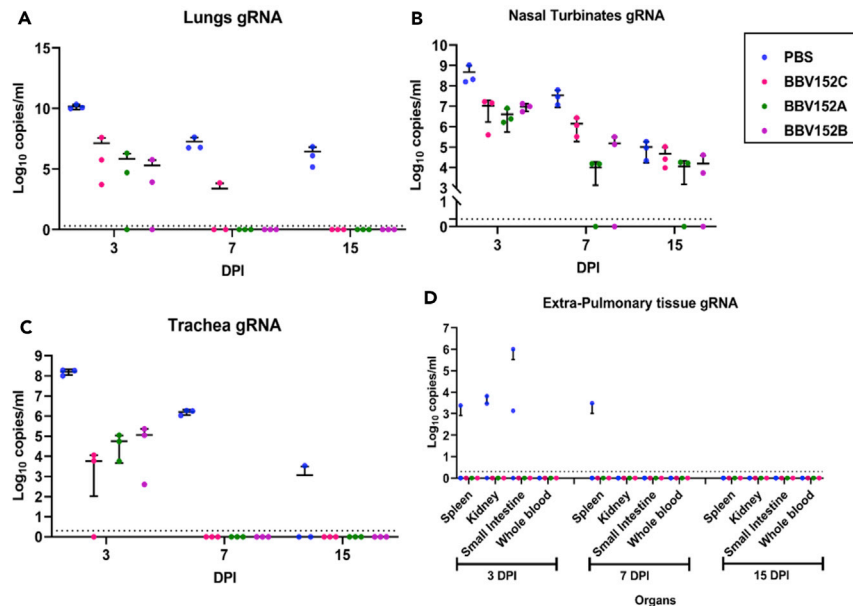
Figure 5. Log$_{10}$ plot of the genomic viral RNA detection in the respiratory tract and extra pulmonary specimens
Genomic viral RNA load in (A) lung, (B) nasal turbinates, (C) trachea, (D) extra pulmonary organs at 3, 7, and 15 DPI. Mean along with standard deviation (SD) is depicted in the scatterplot. The statistical significance was assessed using the Kruskal-Wallis test followed by the two-tailed Mann-Whitney test between the two groups; p values less than 0.05 were considered to be statistically significant. The dotted lines indicate the limit of detection of the assay.

similar to the study reports of Ganneru et al. (2020) in mice. A limitation of this study is that we could not assess the cross-neutralizing ability of this NAb with other related virus like SARS-CoV. Recent studies have reported the existence of broad cross-neutralizing epitopes within lineage B and the cross-neutralizing ability of two SARS-CoV NAb to neutralize SARS-CoV-2 (Lv et al., 2020).

We identified the IgG subclasses induced by BBV152A, BBV152B, and BBV152C and found a predominant IgG$_2$ response with an increasing trend during the immunization and post challenge phase in hamsters. Studies in mice model with the same vaccine candidate have shown a distinct Th$_1$ biased response with a higher average ratio of IgG$_{2a}$/IgG$_1$ especially with the Algel + IMDG group (Ganneru et al., 2020).

Compared to the placebo group, rapid virus clearance was observed in the vaccinated groups from the respiratory tract except for nasal turbinates. We observed the viral gRNA persistence in the nasal turbinates till day 15 in all groups, but the gRNA copy number was lower in vaccinated groups compared to placebo. Many SARS-CoV-2 vaccines in development also reported the absence or partial clearance of virus from the upper respiratory tract (van Doremalen et al., 2020; Yu et al., 2020). Upper and lower respiratory tract protection is thought to be mainly mediated by the secretory IgA and IgG, respectively (Reynolds, 1988; Holmgren and Czerkinsky, 2005). Intramuscular vaccinations generally lead to antigen-specific systemic humoral and cell-mediated immune responses, but their ability to induce mucosal immunity is poor (Krammer, 2020). There are also reports of parenteral vaccine-induced mucosal responses in humans and experimental animal models (Clements and Freytag, 2016). Mucosal immune responses were not studied in the current experiment.

The inactivated vaccine candidates BBV152A, BBV152B, and BBV152C studies in rhesus macaque showed complete clearance of virus by 7 DPI in respiratory organs (Yadav et al., 2020). Dose-related difference in viral clearance was observed in other inactivated vaccine candidates like PiCOvacc and BBIBP-CorV, where lower dose groups were found less effective in clearance (Gao et al., 2020; Wang et al., 2020). Gross and histopathological examination of the lungs of the placebo group had evidence of interstitial pneumonia in the placebo group on 3 and 7 DPI. However, vaccinated groups had no evidence of gross and histopathological changes indicating the protective efficacy of these inactivated vaccine candidates. Lower viral load, absence of lung pathology, and high titers of neutralizing antibodies post-infection demonstrate the protective efficacy of BBV152A, BBV152B, and BBV152C in immunized hamsters, and of these three candidates, BBV152A showed the better response.
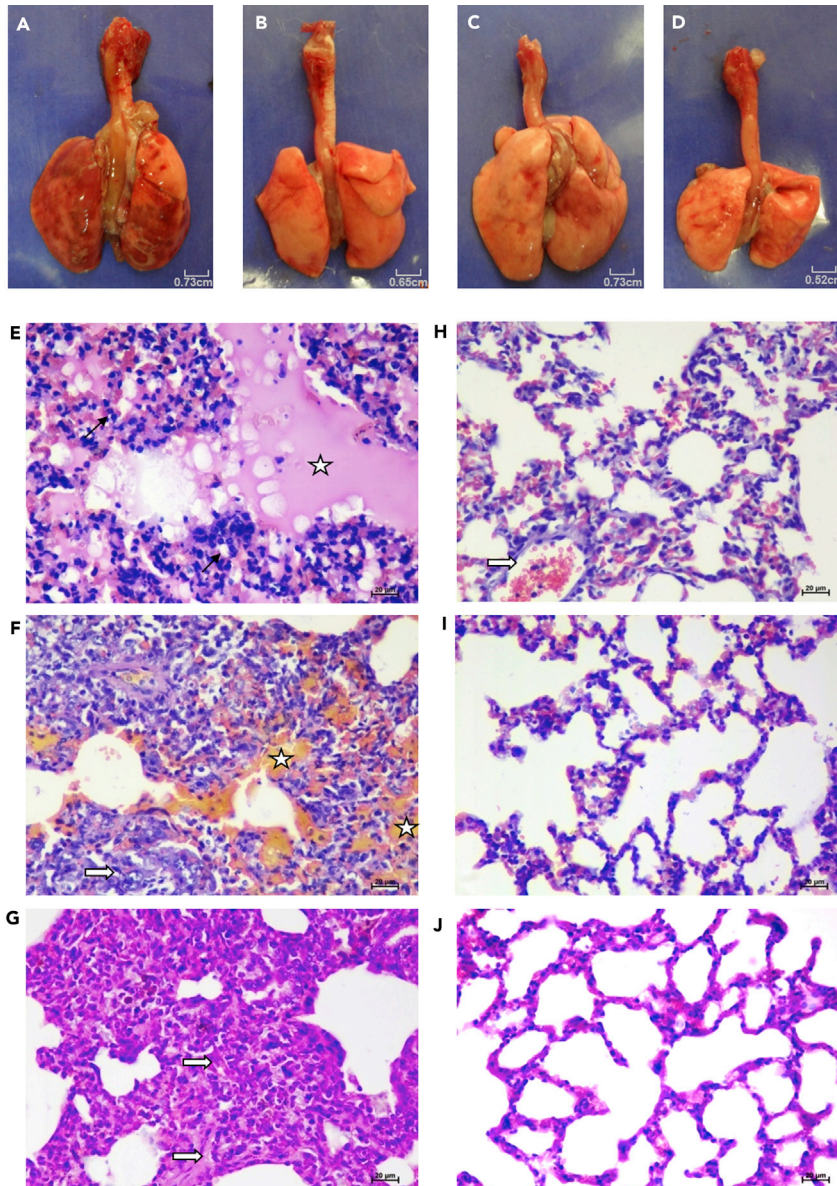
Figure 6. Gross and histopathological observations of lungs in hamsters after virus inoculation

(A–D) (A) Lungs of hamster from group I on 7 DPI showing diffuse areas of consolidation and congestion in the left and right lower lobe with few congestive foci in right upper lobe, scale bar = 0.73cm. Lungs from (B) group II, scale bar = 0.65cm (C) group III, scale bar = 0.73cm and (D) group IV showing normal gross appearance on 7 DPI scale bar = 0.52cm.

(E) Lung tissue from group I on 3 DPI showing acute inflammatory response with diffuse alveolar damage, haemorrhages, inflammatory cell infiltration (black arrow), hyaline membrane formation (white arrow), and accumulation of eosinophilic edematous exudate (star), scale bar = 20μm.

(F) Lung tissue of group I on 7 DPI showing acute interstitial pneumonia with marked alveolar damage, thickening of alveolar and accumulation of mononuclear cells, and macrophages (white arrow), and lysed erythrocytes in the alveolar luminal space (star), scale bar = 20μm.

(G–J) (G) Lung tissue from group I on 15 DPI depicting interstitial pneumonia with marked thickening of alveolar septa with type-II pneumocyte hyperplasia and fibro-elastic proliferation with collagen deposition at alveolar epithelial lining (white arrow), scale bar = 20μm. Lung section from group II showing no evidence of disease (H) on 3 DPI few congestive foci, scale bar = 20μm (I) on 7 DPI, scale bar = 20μm (J) on 15 DPI, scale bar = 20μm.
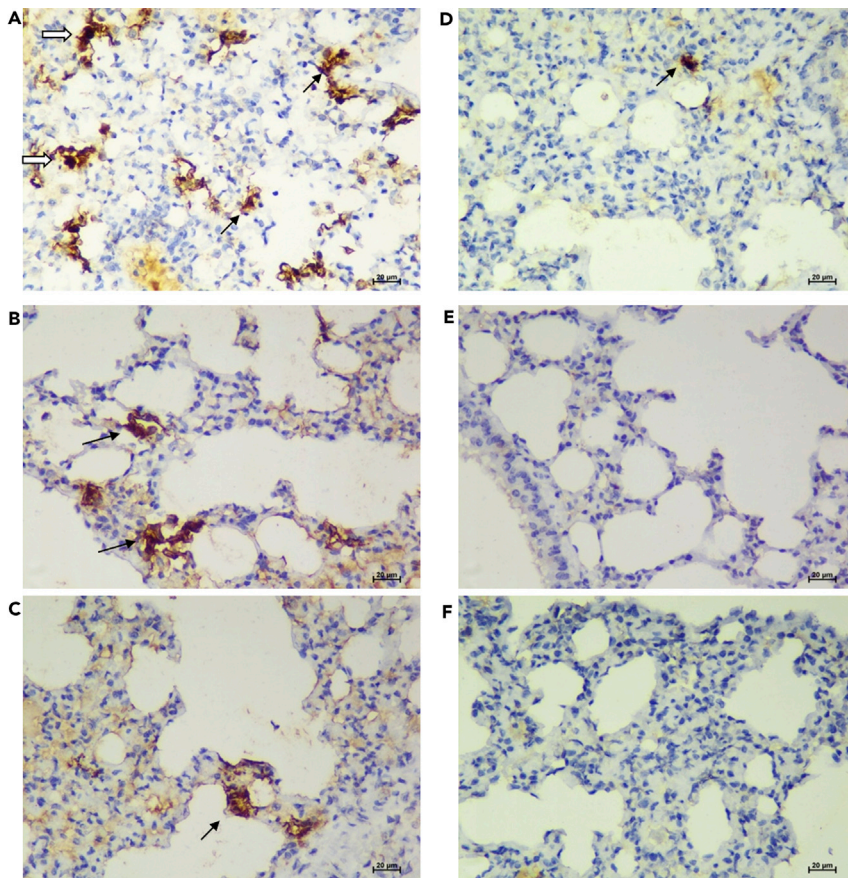
Figure 7. Immunohistochemistry findings in lungs of hamsters after virus challenge

Left panel depicts group treated with placebo and the right panel shows vaccinated group II animals. Lung section from group I showing viral antigen (A) on 3 DPI in alveolar type-II pneumocytes (*black* arrow) and in alveolar macrophages (*white* arrow), scale bar = 20μm (B) on 7 DPI in alveolar type-II pneumocytes (*black arrow*), scale bar = 20μm (C) on 15 DPI in type-II alveolar pneumocytes (*black arrow*), scale bar = 20μm. Lung section from group II showing viral antigen (D) on 3 DPI in alveolar macrophages (*black arrow*), scale bar = 20μm (E) on 7 DPI in alveolar epithelium and alveolar macrophages, scale bar = 20μm (F) on 15 DPI in the alveolar epithelium and alveolar macrophages, scale bar = 20μm.

Limitations of the study

The cross-neutralizing potential of the NAb with other SARS CoV-2 clades, longevity of the antibody response, and the cell-mediated immune response elicited by vaccine candidates needs to be explored further.

Resource availability

Lead contact

Further information and requests for resources and reagents should be directed to the lead contact, Dr. Pragya D Yadav, Scientist 'E' and group Leader, Maximum Containment Facility, Indian Council of Medical Research-National Institute of Virology, Pune at (hellopragya22@gmail.com).

Materials availability

This study did not generate new unique reagents.

Data and code availability

The published article includes all data sets generated or analyzed during this study.

METHODS

All methods can be found in the accompanying Transparent Methods supplemental file.

AUTHOR CONTRIBUTIONS

PDY, SM, KM, PA, NG, and BB conceived and designed the study. KME, RE, VKS, and SDP performed vaccine design and production. PDY and SM performed the planning of animal experiments. SM, PDY, MK, AK, and CM performed the animal experimentation. PDY, AS, GS, GD, DN, and DYP performed the laboratory work planning and data analysis. GD, SP, RJ, TM, SS, and PS performed sample processing in the laboratory. PDY, SM, DN, AS, and DYP have drafted the manuscript. PDY, SM, AS, DYP, KM, PA, NG, SP, and BB substantively revised it. All authors reviewed the manuscript and agree to its contents.

DECLARATION OF INTERESTS

REFERENCES

Addetia, A., Crawford, K.H., Dingens, A., Zhu, H., Roychoudhury, P., Huang, M.L., Jerome, K.R., Bloom, J.D., and Greninger, A.L. (2020). Neutralizing antibodies correlate with protection from SARS-CoV-2 in humans during a fishery vessel outbreak with a high attack rate. J. Clin. Microbiol. 58, e02107–e02120, https://doi.org/10.1128/JCM.02107-20.

Chan, J.F., Zhang, A.J., Yuan, S., Poon, V.K., Chan, C.C., Lee, A.C., Chan, W.M., Fan, Z., Tsoi, H.W., Wen, L., and Liang, R. (2020). Simulation of the clinical and pathological manifestations of Coronavirus Disease 2019 (COVID-19) in golden Syrian hamster model: implications for disease pathogenesis and transmissibility. Clin. Infect. Dis. Mar. 26, ciaa325.

Clements, J.D., and Freytag, L.C. (2016). Parenteral vaccination can be an effective means of inducing protective mucosal responses. Clin. Vaccin. Immunol. 23, 438–441.

Docea, A.O., Tsatsakis, A., Albulescu, D., Cristea, O., Zlatian, O., Vinceti, M., Moschos, S.A., Tsoukalas, D., Goumenou, M., Drakoulis, N., and Dumanov, J.M. (2020). A new threat from an old enemy: Re-emergence of coronavirus. Int. J. Mol. Med. 45, 1631–1643.

Ganneru, B., Jogdand, H., Dharam, V.K., Molugu, N.R., Prasad, S.D., Vellimudu, S., Ella, K.M., Ravikrishnan, R., Awasthi, A., Jose, J., and Rao, P. (2020). Evaluation of Safety and Immunogenicity of an Adjuvanted, TH-1 Skewed, Whole Virion Inactivated SARS-CoV-2 Vaccine-Bbv152 (bioRxiv). https://doi.org/10.1101/2020.09.09.285445.

Gao, Q., Bao, L., Mao, H., Wang, L., Xu, K., Yang, M., Li, Y., Zhu, L., Wang, N., Lv, Z., and Gao, H. (2020). Development of an inactivated vaccine candidate for SARS-CoV-2. Science 369, 77–81, https://doi.org/10.1126/science.abc1932.

Goumenou, M., Sarigiannis, D., Tsatsakis, A., Anesti, O., Docea, A.O., Petrakis, D., Tsoukalas, D., Kostoff, R., Rakitskii, V., Spandidos, D.A., and Aschner, M. (2020). COVID-19 in Northern Italy: an integrative overview of factors possibly influencing the sharp increase of the outbreak. Mol. Med. Rep. 22, 20–32.

Holmgren, J., and Czerkinsky, C. (2005). Mucosal immunity and vaccines. Nat. Med. 11, S45–S53.

Imai, M., Iwatsuki-Horimoto, K., Hatta, M., Loeber, S., Halfmann, P.J., Nakajima, N., Watanabe, T., Ujie, M., Takahashi, K., Ito, M., et al. (2020). Syrian hamsters as a small animal model for SARS-CoV-2 infection and countermeasure development. Proc. Natl. Acad. Sci. 117, 16587–16595.

Islam, M.T., Nasiruddin, M., Khan, I.N., Mishra, S.K., Kudrat-E-Zahan, M., Riaz, T.A., Ali, E.S., Rahman, M.S., Mubarak, M.S., Martorell, M., and Cho, W.C. (2020). A perspective on emerging therapeutic interventions for COVID-19. Front. Public Health 8, 281.

Krammer, F. (2020). SARS-CoV-2 vaccines in development. Nature 586, 516–527.

Li, Q., Guan, X., Wu, P., Wang, X., Zhou, L., Tong, Y., Ren, R., Leung, K.S.M., Lau, E.H.Y., and Wong, J.Y. (2020). Early transmission dynamics in Wuhan, China, of novel coronavirus–infected pneumonia. N. Engl. J. Med. 382, 1199–1207.

Luan, J., Lu, Y., Jin, X., and Zhang, L. (2020). Spike protein recognition of mammalian ACE2 predicts the host range and an optimized ACE2 for SARS-CoV-2 infection. Biochem. Biophys. Res. Commun. 526, 165–169.

Lv, Z., Deng, Y.Q., Ye, Q., Cao, L., Sun, C.Y., Fan, C., Huang, W., Sun, S., Sun, Y., Zhu, L., et al. (2020). Structural basis for neutralization of SARS-

CoV-2 and SARS-CoV by a potent therapeutic antibody. Science *369*, 1505–1509.

Mohandas, S., Jain, R., Yadav, P.D., Shete-Aich, A., Sarkale, P., Kadam, M., Kumar, A., Deshpande, G., Baradkar, S., Patil, S., et al. (2020). Evaluation of the susceptibility of mice & hamsters to SARS-CoV-2 infection. Indian J. Med. Res. *151*, 479.

Pandey, S.C., Pande, V., Sati, D., Upreti, S., and Samant, M. (2020). Vaccination strategies to combat novel corona virus SARS-CoV-2. Life Sci. *256*, 117956.

Phan, L.T., Nguyen, T.V., Luong, Q.C., Nguyen, T.V., Nguyen, H.T., Le, H.Q., Nguyen, T.T., Cao, T.M., and Pham, Q.D. (2020). Importation and human-to-human transmission of a novel coronavirus in Vietnam. N. Engl. J. Med. *382*, 872–874.

Reynolds, H.Y. (1988). Immunoglobulin G and its function in the human respiratory tract. Mayo Clinic Proc. *63*, 161–174.

Roberts, A., Vogel, L., Guarner, J., Hayes, N., Murphy, B., Saki, S., and Subbarao, K. (2005). Severe acute respiratory syndrome coronavirus infection of golden Syrian hamsters. J.Virol. *79*, 503–511.

Rogers, T.F., Zhao, F., Huang, D., Beutler, N., Burns, A., He, W.T., Limbo, O., Smith, C., Song, G., Woehl, J., and Yang, L. (2020). Isolation of potent SARS-CoV-2 neutralizing antibodies and protection from disease in a small animal model. Science *369*, 956–963.

Sanders, B., Koldijk, M., and Schuitemaker, H. (2015). Inactivated viral vaccines. In Vaccine Analysis: Strategies, Principles, and Control (Springer), pp. 45–80.

Sia, S.F., Yan, L.M., Chin, A.W., Fung, K., Choy, K.T., Wong, A.Y., Kaewpreedee, P., Perera, R.A., Poon, L.L., Nicholls, J.M., et al. (2020). Pathogenesis and transmission of SARS-CoV-2 in golden hamsters. Nature *583*, 834–838.

The Centre for Evidence-Based Medicine. (2020). Global Covid-19 case fatality rates. https://www.cebm.net/covid-19/global-covid-19-case-fatality-rates/.

Tostanoski, L.H., Wegmann, F., Martinot, A.J., Loos, C., McMahan, K., Mercado, N.B., Yu, J., Chan, C.N., Bondoc, S., Starke, C.E., and Nekorchuk, M. (2020). Ad26 vaccine protects against SARS-CoV-2 severe clinical disease in hamsters. Nat. Med *26*, 1694–1700.

Tsatsakis, A., Calina, D., Falzone, L., Petrakis, D., Mitrut, R., Siokas, V., Pennisi, M., Lanza, G., Libra, M., Doukas, S.G., and Doukas, P.G. (2020). SARS-CoV-2 pathophysiology and its clinical implications: an integrative overview of the pharmacotherapeutic management of COVID-19. Food Chem. Toxicol. *146*, 111769.

van Doremalen, N., Lambe, T., Spencer, A., Belij-Rammerstorfer, S., Purushotham, J.N., Port, J.R., Avanzato, V.A., Bushmaker, T., Flaxman, A., Ulaszewska, M., et al. (2020). ChAdOx1 nCoV-19 vaccine prevents SARS-CoV-2 pneumonia in rhesus macaques. Nature *586*, 578–582.

Wang, H., Zhang, Y., Huang, B., Deng, W., Quan, Y., Wang, W., Xu, W., Zhao, Y., Li, N., Zhang, J., et al. (2020). Development of an inactivated vaccine candidate, BBIBP-CorV, with potent protection against SARS-CoV-2. Cell *182*, 713–721.

Wang, Y., Miao, J., Chard, L., and Wang, Z. (2019). Syrian hamster as an animal model for the study on infectious diseases. Front. Immunol. *10*, 2329.

Wilder-Smith, A., Chiew, C.J., and Lee, V.J. (2020). Can we contain the COVID-19 outbreak with the same measures as for SARS? Lancet Infect. Dis. *20*, E102–E105.

World Health Organization. (2020a). Coronavirus disease (COVID-19) outbreak situation. https://www.who.int/emergencies/diseases/novel-coronavirus-2019.

World Health Organization. (2020b). Draft Landscape of COVID-19 Candidate Vaccines, 28 August 2020. https://www.who.int/who-documents-detail/draft-landscape-of-covid-19-candidate-vaccines.

Yadav, P., Ella, R., Kumar, S., Patil, D., Mohandas, S., Shete, A., Bhati, G., Sapkal, G., Kaushal, H., Patil, S., et al. (2020). Remarkable immunogenicity and protective efficacy of BBV152, an inactivated SARS-CoV-2 vaccine in rhesus macaques. Res. Square. https://doi.org/10.21203/rs.3.rs-65715/v1.

Yu, J., Tostanoski, L.H., Peter, L., Mercado, N.B., McMahan, K., Mahrokhian, S.H., Nkolola, J.P., Liu, J., Li, Z., Chandrashekar, A., and Martinez, D.R. (2020). DNA vaccine protection against SARS-CoV-2 in rhesus macaques. Science *369*, 806–811.

Supplemental Information

Immunogenicity and protective efficacy

of BBV152, whole virion inactivated SARS- CoV-2

vaccine candidates in the Syrian hamster model

Sreelekshmy Mohandas, Pragya D. Yadav, Anita Shete-Aich, Priya Abraham, Krishna Mohan Vadrevu, Gajanan Sapkal, Chandrashekhar Mote, Dimpal Nyayanit, Nivedita Gupta, Vellimedu Kannappa Srinivas, Manoj Kadam, Abhimanyu Kumar, Triparna Majumdar, Rajlaxmi Jain, Gururaj Deshpande, Savita Patil, Prasad Sarkale, Deepak Patil, Raches Ella, Sai D. Prasad, Sharda Sharma, Krishna M. Ella, Samiran Panda, and Balram Bhargava

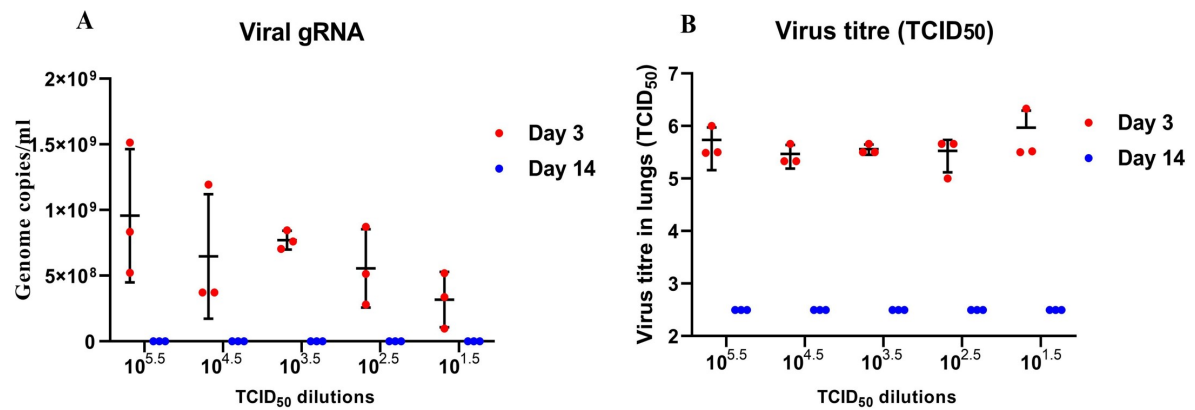**Supplementary figures and legends**

Figure S1. [Graph showing A) viral gRNA copy number and B) virus titre in lungs samples of hamsters challenged with various dilutions of virus for intranasal dose optimization for challenge study on 3 and 14 DPI.] Related to Figure 1.

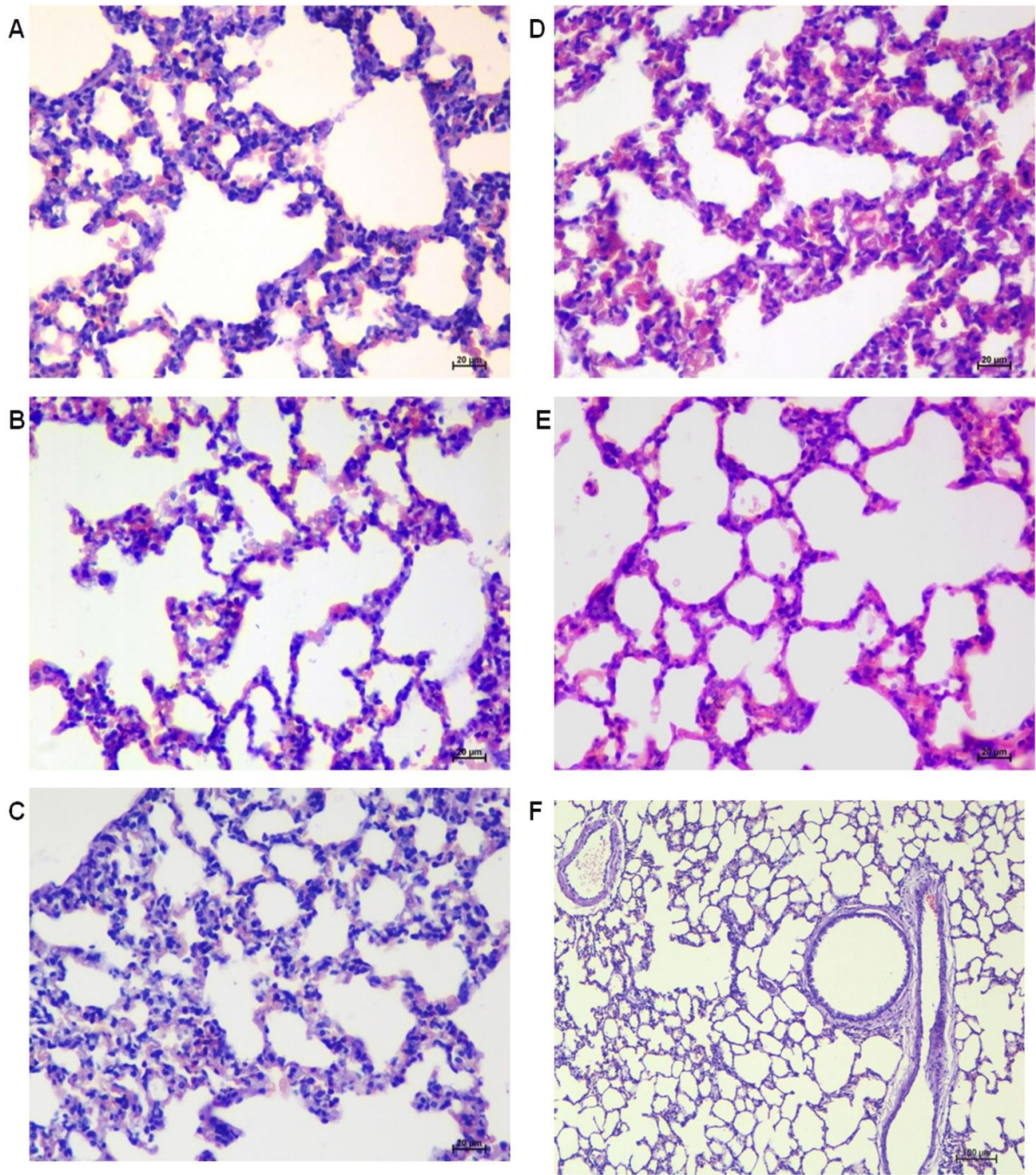**Figure S2.** [Histopathological observations of lungs in group III **A)** on 3 DPI, scale bar = 20μm **B)** on 7DPI, scale bar = 20μm and **C)** on 15 DPI, scale bar = 20μm and group IV hamsters **D)** on 3 DPI, scale bar = 20μm **E)** 7 DPI, scale bar = 20μm **F)** and on 15 DPI, scale bar = 100μm.] Related to Figure 6.
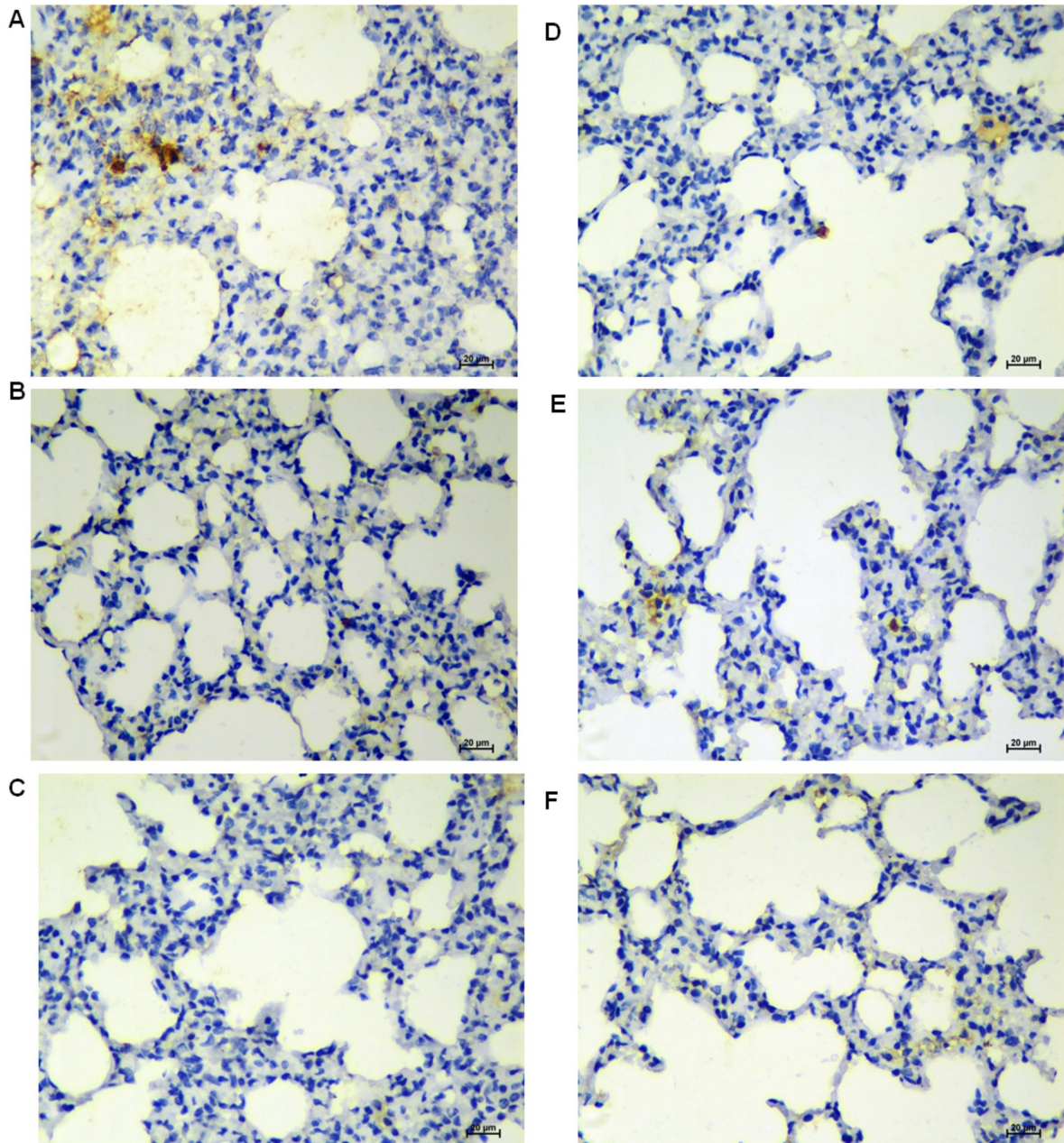
Figure S3. [Immunohistochemistry findings in lungs of group III showing **A)** focal positivity on 3 DPI, scale bar = 20μm **B)** absence of antigen on 7DPI, scale bar = 20μm and **C)** on 15 DPI, scale bar = 20μm and group IV hamsters **D)** focal positivity on 3 DPI, scale bar = 20μm **E)** absence of antigen on 7DPI, scale bar = 20μm **F)** and on 15 DPI, scale bar = 20μm.] Related to Figure 7.

Figure S4. [Cytokine profile for (A) TNF- α(B) IL-4 (C) IL-10(D) IL-6 (E) IFN γ(F) IL-12

at 3,7 and 15 DPI. The statistical significance was assessed using the Kruskal-Wallis

test followed by the two-tailed Mann-Whitney test between the two groups; p-values

less than 0.05 were considered to be statistically significant.] Related to Figure 1.

.

Transparent Methods

Key Resource table

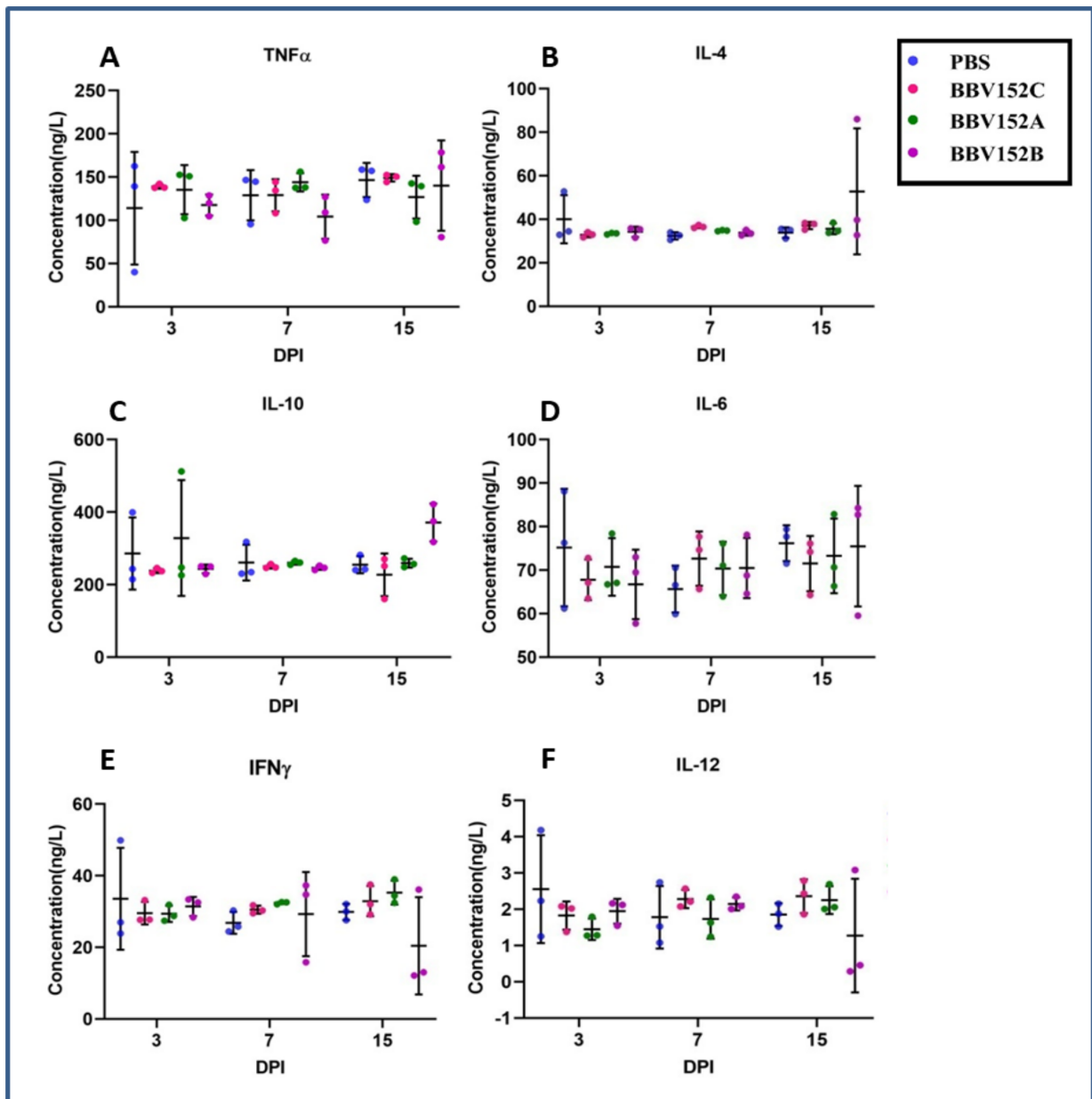| Reagent/Resource	Source	Identifier
Experimental models: Cell lines		
Vero CCL-81	ATCC	Cat#ATCC-CCL-81
Experimental models: Organisms/strains		
Hamsters: Syrian hamsters	Indian Council of Medical Research-National Institute of Nutrition, Hyderabad, India	N/A
Virus strain		
NIV-2020-770	ICMR-National Institute of Virology, Pune	"GISAID: hCoV 19/India/770/2020| EPI_ ISL_ 420545|" "GISAID: hCoV19/India/2020770/2020|EPI_ISL_420546|"
Antibodies		
Biotin mouse anti-Armenian and Syrian Hamster IgG1	BD Biosciences	Cat#554007
Biotin mouse anti-Armenian and Syrian Hamster IgG2	BD Biosciences	Cat#554025
Anti-mice HRP	Dako	Cat #P044701-2
Chemicals		
Imidazoquinoline	Viro Vax	N/A
Alum	Brenntag	N/A

β-Propionolactone	Ferak	N/A
Minimum Essential Medium (MEM)	Thermo Fisher Scientific	Cat # 11534466
Dulbecco's Modified Eagle Medium	Sigma-Aldrich	Cat # D5796
Foetal Bovine serum	Sigma-Aldrich	Cat # F4135
Penicillin/Streptomycin	Sigma-Aldrich	Cat # P4333
Skimmed milk powder	Difco	Cat #232100
3,3′,5,5′-Tetramethylbenzidine (TMB) substrate	Clinical science product	Cat#01016-1-1000
Critical Commercial Assays		
Hamster Interleukin ELISA Kit	Immunotag	Cat #ITE150025, ITE150027, ITE150010, ITE150004, ITE150058, ITE150028, ITE15003 0
MagMAX™ Viral/Pathogen Nucleic Acid Isolation Kit	Thermo Fisher Scientific	Cat #A42352
Software		
PRISM	GraphPad software	Version 8
BioRender	BioRender software	N/A

Experiment model and subject details

Cells and virus

Vero CCL-81 cells were grown in Minimum Essential Media (MEM) (Thermo fisher

Scientific, USA) supplemented with 2% foetal bovine serum (FBS) (Sigma-Aldrich,

USA). SARS-CoV-2 strain, NIV-2020-770 isolated from a patient's throat/ nasal swab sample at Indian Council of Medical Research- National Institute of Virology (ICMR-NIV), Pune was passaged up to three times in Vero CCL81 cells before use[1]. The infectious virus titre was found to be $10^{6.5}$ tissue culture infective dose 50 ($TCID_{50}$)/ml.

Ethics statement

The study was approved by the Institutional Project Review Committee, Institutional Animal Ethics Committee and Institutional Biosafety Committee of ICMR-NIV, Pune. All the experiments were performed as per the guidelines laid down by the Committee for the Purpose of Control and Supervision of Experiments in Animals[2].

Immunization of hamsters

Thirty-six, 6- 8 week old female Syrian hamsters were divided into four groups, viz., Group I, II, III and IV of 9 hamsters each. The hamsters were housed in individually ventilated cages with *ad libitum* food and water. Group I was administered with phosphate-buffered saline (PBS), group II with BBV152C (6µg of vaccine candidate along with Algel), group III with BBV152A (3µg of vaccine candidate with Algel-IMDG) and group 4 with BBV152B (3µg of vaccine candidate with Algel-IMDG). Animals of each group were immunized with 0.1 ml of PBS/vaccine formulations intramuscularly in the hind leg under isoflurane anaesthesia on 0, 14 and 35 days. Post immunization hamsters were observed daily for clinical signs and injection site reactions. Rectal temperature was monitored every 24 hours for 3 days post-immunization and weekly thereafter. Body weight was measured every alternate day for the first week and weekly thereafter. The hamsters were bled on days 12, 21 and 48 post-immunization to check for antibody response.

Dose optimization study in hamsters

For optimization of the intranasal virus challenge dose, SARS-CoV-2 dilutions ranging from $10^{1.5}$ $TCID_{50}$/0.1ml to $10^{5.5}$ $TCID_{50}$/0.1ml were inoculated in 5 groups of 6 Syrian hamsters each in containment facility. Three hamsters from each group were sacrificed on days 3 and 14 post-inoculation to check for viral load in the lungs by real-time RT-PCR/virus titration and lung pathology.

Challenge study in immunized hamsters

The immunized hamsters were challenged with 0.1 ml of $10^{5.5}$ $TCID_{50}$ SARS-CoV-2 virus intranasally on the eighth-week post-immunization (day 50) in the containment facility of ICMR-National Institute of Virology, Pune under isoflurane anaesthesia. Throat swabs were collected in 1 ml virus transport media on every alternate day post-inoculation for viral load estimation. Three hamsters from each group were euthanized on 3, 7 and 15 DPI to collect throat swab, nasal wash, rectal swab, blood and organ samples for viral RNA estimation, titration, histopathology, and immunological analysis.

Method details

Inactivated SARS-CoV-2 whole virion vaccine

SARS-CoV-2 strain (NIV-2020-770) isolated at ICMR-NIV, Pune was propagated in Vero CCL81 cells and harvested on observation of cytopathic effect in the cells. At Bharat Biotech International Limited (BBIL), further candidate preparation was performed. BPL (Ferak, Germany) was added to the virus harvest following filtration and stabilization of the harvest using a buffer. The mixture was kept at 2-8°C with continuous stirring for 24 hrs and was further hydrolysed by incubating at 37°C for

2hrs. Column chromatography was used for further purification and the process intermediate was concentrated to prepare the whole virion vaccine. Two different antigen concentrations (3 μg and 6 μg) and 2 adjuvants namely Algel (Aluminium hydroxide) and Algel-IMDG (TLR 7/8 agonist adsorbed alum) in combinations were used for the study. The vaccine formulations evaluated in the study were 6 μg with Algel (BBV152C), 3 μg with Algel-IMDG (BBV152A) and 6 μg with Algel-IMDG (BBV152B).

Enzyme-linked Immunosorbent Assay (ELISA)

Ninety-six well microtitre plates were coated with 1:10 diluted inactivated SARS-CoV-2 antigen with carbonate buffer (pH 9.5) overnight at 4 °C. Subsequently, wells were blocked with liquid plate sealer (CANDOR Bioscience GmbH, Germany) for two hours at room temperature (25-30°C). The wells were washed 5 times with phosphate-buffered saline with 0.05% Tween 20 (PBS-T) and were incubated at 37°C for one hour with 100μl of diluted hamster serum samples (1: 100). Negative control was added to each plate. After 5 washes with PBS-T, anti-hamster IgG antibodies 1:3000 (Thermoscientific, USA) were added and incubated for 1 hour at 37°C. Following 5 washes with PBS-T, 100 μl of substrate, 3',3'5,5'-tetramethylbenzidine (TMB) was added to each well. The colour reactions were developed for 10 minutes and after termination, absorbance was measured at 450 nm. Serum IgG titres were determined by testing serial 10-fold dilutions of each sample, starting from 1:100 dilution. Titre values were determined as the highest dilution at which the optical density was more than 0.2 and positive/negative (P/N) ratio above 1.5.

For antibody sub-typing, plates were coated with antigen and blocked as described earlier. Hamster serum, 1:100 diluted in 1% bovine serum albumin in 1× PBST was added to each well and incubated for 1 hour at 37°C. After washing the plates 5 times

with 1× PBST wells were probed with biotinylated anti-Syrian hamster IgG_1 /IgG_2 antibodies diluted at 1:10000 (BD biosciences, USA) and incubated for 1 hour at 37°C. After washing, the plates were incubated with Streptavidin-horse radish peroxidase (HRP) 1:8000 (Thermo-scientific, USA) for 30 minutes at 37°C. The reaction was read as described earlier.

Plaque Reduction Neutralization test (PRNT)

The PRNT assay was performed as described earlier[3]. Briefly, a four- fold serial dilution of hamster serum samples was mixed with an equal amount of virus suspension and incubated at 37°C for 1 hour. Further 0.1 ml of the mixture was inoculated in a 24-well tissue culture plate containing a confluent monolayer of Vero CCL-81 cells. The plate was incubated at 37°C for 60 min and overlay medium (2% carboxymethyl cellulose with 2% FBS in 2X MEM) was added to the cell monolayer, which was further incubated at 37°C in 5% CO2 incubator for 4-5 days and PRNT $_{50}$ titres were calculated.

Cytokine analysis

The serum cytokine levels (TNF-α, IFN-γ, IL-4, IL-6, IL-10 and IL-12) were assessed in hamsters post challenge at 3, 7 and 15 days. A commercial ELISA (Immunotag, USA) was used for the hamster specific cytokine quantitation. For this, plates pre-coated with hamster specific cytokine antibody were used and a streptavidin based HRP system was used for detection and the absorbance was measured at 450 nm.

Real-time RT-PCR for detection of genomic and subgenomic viral RNA

Nasal wash, throat swab and rectal swab samples were collected in 1ml viral transport medium and weighed organ samples (lungs, nasal turbinate, trachea, spleen, kidney and intestine) were triturated in 1 ml sterile tissue culture media, using a tissue

homogenizer (Eppendorf, Germany) and 200 µl of the homogenate/ swab specimens were used for further RNA extraction using MagMAX™ Viral/Pathogen Nucleic Acid Isolation Kit as per the manufacturer's instructions. Real-time RT-PCR was performed for E and RdRp2 gene for SARS-CoV-2 as well as for detection of sgRNA of E gene using published primers[4,5.]

Virus titration

The lungs and nasal turbinate samples from 3, 7 and 15 DPI were used for virus titration in Vero CCL81 cells. 100 µl of the sample was added onto a 24-well plate with Vero CCL81 monolayers and incubated for one hour at 37°C. The media was removed and the cell monolayer was washed with PBS. The plate was incubated with maintenance media with 2% FBS in a CO2 incubator. The plate was examined daily for any cytopathic effects (CPE) using an inverted microscope (Nikon, Eclipse Ti, Japan). The culture supernatant from the wells showing CPE was confirmed by real-time RT-PCR.

Histopathology and immunohistochemistry

Lungs samples collected during necropsy were fixed in 10% neutral buffered formalin. The tissues were processed by routine histopathological techniques for hematoxylin and eosin staining. Duplicate sections were taken for immunohistochemical evaluation. An in-house developed anti-SARS-CoV-2 mouse polyclonal serum was used as the primary antibody for detection. The tissue sections were rehydrated and antigen retrieval was performed using 0.3% hydrogen peroxide in methanol. The slides were incubated with 1: 500 dilution of primary antibody for an hour and an anti-mouse HRP antibody (Dako, USA) was used as a secondary antibody. For detection,

3, 3'-diaminobenzidine tetrahydrochloride substrate, and hydrogen peroxide were used.

Data analysis

For analysis of the data, Graphpad Prism version 8.4.3 software was used. The statistical significance was assessed using the Kruskal-Wallis test Dunn's multiple comparisons test. Two-tailed Mann-Whitney test was performed between the control and the vaccinated groups if the p-value for the Kruskal-Wallis test was found to be significant; p-values less than 0.05 were considered to be statistically significant.

References

1. Sarkale P, Patil S, Yadav PD, Nyayanit DA, Sapkal G, Baradkar S, Lakra R, Shete-Aich A, Prasad S, Basu A, Dar L. First isolation of SARS-CoV-2 from clinical samples in India. Indian Journal of Medical Research. 2020 Feb 1;151(2):244.

2. CPCSEA, 2003. CPCSEA guidelines for laboratory animal facility. Indian J. Pharmacol. 35, 257–274.

3. Deshpande GR, Sapkal GN, Tilekar BN, Yadav PD, Gurav Y, Gaikwad S, Kaushal H, Deshpande KS, Kaduskar O, Sarkale P, Baradkar S. Neutralizing antibody responses to SARS-CoV-2 in COVID-19 patients. Indian Journal of Medical Research. 2020 Jan 1;152(1):82.

4. Choudhary ML, Vipat V, Jadhav S, Basu A, Cherian S, Abraham P, Potdar VA. Development of in vitro transcribed RNA as positive control for laboratory diagnosis of SARS-CoV-2 in India. The Indian Journal of Medical Research. 2020 Feb;151(2-3):251.

5. Wölfel R, Corman VM, Guggemos W, Seilmaier M, Zange S, Müller MA, Niemeyer D, Jones TC, Vollmar P, Rothe C, Hoelscher M. Virological assessment of hospitalized patients with COVID-2019. Nature. 2020 May;581(7809):465-9.

List of abbreviations and their full form

Abbreviations	Full form
SARS-CoV-2	Severe acute respiratory syndrome coronavirus-2
WHO	World Health Organization
COVID-19	Coronavirus disease-19
HCoV	Human coronavirus
SARS-CoV	Severe acute respiratory syndrome coronavirus
MERS-CoV	Middle East Respiratory Syndrome coronavirus
SARS	Severe acute respiratory syndrome
MERS	Middle East Respiratory Syndrome
BPL	β-Propiolactone
TCID50	Median Tissue Culture Infectious Dose
DPI	Day post infection
NAb	Neutralizing antibody
gRNA	Genomic RNA
sgRNA	Subgenomic RNA
TS	Throat swab
IHC	Immunohistochemistry
SD	Standard deviation
MEM	Minimum Essential Media
FBS	Foetal bovine serum
ICMR-NIV	Indian Council of Medical Research-National Institute of Virology
CPCSEA	Committee for the Purpose of Control and Supervision of Experiments in Animals
PBS	Phosphate-buffered saline
PBS-T	Phosphate-buffered saline with tween

TMB	3',3'5,5'-tetramethylbenzidine
PRNT	Plaque Reduction Neutralization Test
ELISA	Enzyme Linked Immunosorbent Assay
HRP	Horseradish peroxidise
CPE	Cytopathic effect